HHS Public Access

Author manuscript

J Invest Dermatol. Author manuscript; available in PMC 2020 June 01.

Published in final edited form as:

J Invest Dermatol. 2019 June ; 139(6): 1349–1361. doi:10.1016/j.jid.2018.11.024.

Identification of a robust methylation classifier for cutaneous melanoma diagnosis

Kathleen Conway[1,2,3], **Sharon N. Edmiston**[3], **Joel S. Parker**[3,4], **Pei Fen Kuan**[5], **Yi-Hsuan Tsai**[3], **Pamela A. Groben**[2,6], **Daniel C. Zedek**[2,6], **Glynis A. Scott**[7,8], **Eloise A. Parrish**[3], **Honglin Hao**[2], **Michelle V. Pearlstein**[2], **Jill S. Frank**[3], **Craig C. Carson**[2], **Matthew D. Wilkerson**[11], **Xiaobei Zhao**[3], **Nathaniel A Slater**[2], **Stergios J. Moschos**[3,10], **David W. Ollila**[3,9], and **Nancy E. Thomas**[2,3]

[1]Department of Epidemiology, School of Public Health, University of North Carolina, Chapel Hill, NC

[2]Department of Dermatology, School of Medicine, University of North Carolina, Chapel Hill, NC

[3]Lineberger Comprehensive Cancer Center (LCCC), University of North Carolina at Chapel Hill, Chapel Hill, NC

[4]Department of Genetics, School of Medicine, University of North Carolina, Chapel Hill, NC

[5]Department of Applied Mathematics and Statistics, Stony Brook University, Stony Brook, NY

[6]Department of Pathology and Laboratory Medicine, School of Medicine, University of North Carolina, Chapel Hill, NC

[7]Department of Dermatology, University of Rochester School of Medicine, Rochester, NY

[8]Department of Pathology and Laboratory Medicine, University of Rochester School of Medicine, Rochester, NY

[9]Department of Surgery, School of Medicine, University of North Carolina, Chapel Hill, NC

[10]Department of Medicine, School of Medicine, University of North Carolina, Chapel Hill, NC

[11]Department of Anatomy, Physiology & Genetics, Uniformed Services University of the Health Sciences, Bethesda, MD

Abstract

Early diagnosis improves melanoma survival, yet the histopathological diagnosis of cutaneous primary melanoma can be challenging even for expert dermatopathologists. Analysis of epigenetic

Corresponding author: Kathleen Conway, Department of Epidemiology, University of North Carolina at Chapel Hill, CB 7435, Chapel Hill, NC 27599. kconway@med.unc.edu.

Disclosure of Potential Conflicts of Interest: No potential conflicts of interest were disclosed

Role of the Sponsors: The sponsors had no role in the design and conduct of the study; in the collection, analysis, and interpretation of data; in the preparation of the manuscript; or in the review or approval of the manuscript. The views expressed in this article are those of the authors and do not reflect the official policy of the Department of Defense or U.S. Government.

alterations, such as DNA methylation, that occur in melanoma can aid in its early diagnosis. Using a genome-wide methylation screen, we assessed CpG methylation in a diverse set of 89 primary invasive melanomas, 73 nevi, and 41 melanocytic proliferations of uncertain malignant potential, classified based on interobserver review by dermatopathologists. Melanomas and nevi were split into training and validation sets. Predictive modeling in the training set using ElasticNet identified a 40-CpG classifier distinguishing 60 melanomas from 48 nevi. High diagnostic accuracy (area under the receiver operator characteristics (ROC) curve (AUC)=0.996, sensitivity=96.6%, and specificity=100.0%) was independently confirmed in the validation set (29 melanomas, 25 nevi) and other published sample sets. The 40-CpG melanoma classifier included homeobox transcription factors and genes with roles in stem cell pluripotency or the nervous system. Application of the 40-CpG melanoma classifier to the diagnostically uncertain samples assigned melanoma or nevus status, potentially offering a diagnostic tool to assist dermatopathologists. In summary, the robust, accurate 40-CpG melanoma classifier offers a promising assay for improving primary melanoma diagnosis.

Keywords

melanoma; nevi; methylation; diagnosis; diagnostic biomarkers

INTRODUCTION

Cutaneous melanoma is an aggressive malignancy with the potential to metastasize early, and there is a pronounced survival difference between localized and metastatic disease (Landow et al., 2017; Shaikh et al., 2016; Siegel et al., 2018; Whiteman et al., 2015). Despite newly available targeted and immunomodulatory agents for the treatment of melanoma (Andtbacka et al., 2015; Clarke et al., 2018; Hodi et al., 2016; Long et al., 2017; Ribas et al., 2016; Ribas et al., 2015; Robert et al., 2015; Schachter et al., 2017), the durability of the response is not yet known and systemic therapies lead to cures in a relatively small number of patients. Therefore, early detection is crucial for favorable outcomes, but early definitive diagnosis can be difficult due to the overlap in clinical and histopathological appearances of melanomas and highly prevalent melanocytic nevi (moles) (Strauss et al., 2007). Histopathological review is the ‘gold standard’ for melanoma diagnosis; however, numerous studies have reported interobserver discordance in the diagnosis of melanocytic lesions even by expert dermatopathologists (Brochez et al., 2002; Elmore et al., 2017; Shoo et al., 2010; Veenhuizen et al., 1997). In one study (Farmer et al., 1996), review of 40 benign and malignant melanocytic lesions by eight dermatopathologists produced discordant diagnoses in 38% of cases. Moreover, certain nevus subtypes, especially dysplastic nevi, Spitz nevi, and atypical blue nevi can be difficult to distinguish from melanoma (Brochez et al., 2002; Gerami et al., 2014). The difficulty in accurately diagnosing melanoma presents a quandary for clinicians, who biopsy and often re-excise with margins large numbers of dysplastic nevi in the population (Fung, 2003), due in part to lack of confidence in the histopathological diagnosis. A critical need exists for improving diagnostic methods to avoid under- and over-treatment of melanocytic lesions. However, the small size of melanocytic lesions and early melanomas, which are typically submitted in their entirety in formalin to the pathologist for diagnosis, present particular challenges as

any new diagnostic test needs to perform reliably on small formalin-fixed paraffin-embedded (FFPE) samples.

Prior studies have shown that melanomas differ from nevi at the molecular level, exhibiting variations in mRNA expression (Alexandrescu et al., 2010; Clarke et al., 2015; Haqq et al., 2005; Koh et al., 2009; Talantov et al., 2005), gene copy number (Bastian et al., 2000; Bastian et al., 2003; Bauer and Bastian, 2006; Gerami et al., 2009; North et al., 2014; Shain et al., 2015), protein expression (Busam, 2013; Ivan and Prieto, 2010; Uguen et al., 2015), and DNA methylation (Conway et al., 2011; Gao et al., 2013; Gao et al., 2014), indicating that certain molecular biomarkers could provide valuable tools for melanoma diagnosis, alone or with histopathology. However, due to the practical limitations of typically small FFPE samples and technical challenges or labor intensity in the performance and implementation of some assays, few molecular differences have been translated to the clinic for melanoma diagnosis.

DNA methylation is a relatively stable epigenetic modification to the DNA that does not alter the nucleotide sequence but is associated with variation in gene expression (Plass, 2002). Changes in methylation at CpG dinucleotides in the upstream regulatory regions of genes are often among the earliest events observed during neoplastic progression of precancerous lesions (Arai and Kanai, 2010), and hypermethylation of CpG islands in tumor suppressor gene promoters is a common mechanism of gene silencing in human cancer (Herman and Baylin, 2003). Aberrant DNA methylation occurs widely in melanomas (Furuta et al., 2004; Hoon et al., 2004), and we (Conway et al., 2011) and others (Gao et al., 2013; Gao et al., 2014) have reported differences in DNA methylation between primary melanomas and nevi, supporting the use of epigenetic biomarkers for early melanoma diagnosis.

Our initial study using a methylation array that targeted cancer-related genes provided proof-of-principle that DNA methylation differences could distinguish invasive primary melanomas from benign nevi in small FFPE samples (Conway et al., 2011; Thomas et al., 2014). In the present study, we extend this work by identifying and independently validating a highly accurate 40-CpG melanoma classifier that distinguishes primary melanomas from a broad histopathologic spectrum of nevi within a set of melanocytic samples reviewed by a panel of expert dermatopathologists. These findings could translate to a robust melanoma diagnostic test ideal for use in FFPE melanocytic samples.

RESULTS

Patient and sample characteristics

Illumina Infinium HumanMethylation450 BeadChip (450K) analysis was successfully performed on 97% of samples tested. The clinicopathologic characteristics of the sample set are included in Table 1. The sample set of FFPE tissues included 89 cutaneous primary invasive melanomas, 73 nevi, and 41 melanocytic proliferations of uncertain malignant potential (‘uncertain’ samples). All melanomas and nevi were classified based on complete consensus between the original pathology report and three dermatopathology reviewers (four interpretations), although we did not exclude a lesion as melanoma if the majority of

dermatopathologists interpreted the lesion as melanoma and visceral metastases and/or death from melanoma provided unequivocal evidence of the malignancy of the lesion. The diagnostically uncertain samples lacked complete consensus between the four interpretations or were called uncertain by any dermatopathologist or the pathology report.

The melanomas had median Breslow thickness of 1.85 millimeters (mm) (range of 0.37–17.00 mm) and were balanced for 7th Edition American Joint Committee on Cancer (AJCC) tumor stages (Balch et al., 2009), and both sample classes were comprised of common and less common histopathological subtypes. The 73 nevi included intradermal, common acquired, dysplastic, Spitz, and blue nevi. The 203 specimens (89 melanomas, 73 nevi, and 41 uncertain samples) were from 202 different patients; one patient had two synchronous primary melanomas, both of which were included in the study. Melanoma patients were more frequently older than nevus patients ($P < 0.001$). Melanomas and nevi (excluding uncertain samples) were randomly divided into training (67% of samples; 60 melanomas and 48 nevi) and validation (33%; 29 melanomas and 25 nevi) sets (Table 1); these did not differ significantly in patient age, sex or other clinical or histopathological characteristics.

Development of a 40-CpG melanoma classifier and validation in an independent test set

Monte-Carlo cross validation via ElasticNet was used to develop and compare the diagnostic accuracy of CpG classifiers derived from multiple Infinium HumanMethylation450 (450K) probe sets in the training set. Inclusion of all CpG probes provided slightly better diagnostic accuracy than a limited set of probes associated with candidate genes identified from our prior study (Conway et al., 2011) (Supplementary Figures S1a-c online). When accounting for age differences in the models by either removing age-associated probes or adjusting for age, or both, each method resulted in a prediction model with inferior diagnostic discrimination; however, this could be overcome by increasing the number of features in the age-adjusted models. Restricting the models to probes showing larger methylation differences (β interquartile range [IQR] > 0.2) between melanomas and nevi (Supplementary Figures S1a and S1b online) and/or to probes with Illumina gene annotation (Supplementary Figure S1d online) produced results very comparable to the more complete probe sets. Based on comparative performance of the models, we identified a 40-CpG melanoma classifier associated with 38 genes for further characterization derived from the probe set filtered for IQR > 0.2 β and with gene annotation (n = 41,448 probes; Supplementary Figure S1d online). CpGs contributing to the 40-CpG melanoma classifier were hypermethylated (n = 23) or hypomethylated (n = 17) in melanomas relative to nevi. The majority of classifier CpGs were located in the upstream regulatory regions of genes (TSS200, TSS1500, 5'UTR), including one-third in enhancer regions (Table 2). Neighboring CpGs around the classifier probes were also similarly differentially methylated in melanomas (Supplementary Figure S2 online).

The heatmap in Figure 1a illustrates the differential methylation at the 40-CpG melanoma classifier probes in primary melanomas and nevi with diagnostic consensus in the training and validation sets. Separate heatmaps for the training and validation sets are also provided in Supplementary Figure S3 online. As shown in Figure 1b, the 40 CpG diagnostic classifier distinguishes all histological subtypes of nevi, including dysplastic and Spitz nevi, from

melanomas. Moreover, early T1a melanomas or thin melanomas with Breslow thickness <1.0 mm were distinguished from nevi (Supplementary Figure S4 online). The diagnostic accuracy of the classifier for melanoma in the independent validation set was high (AUC = 0.996), with a sensitivity of 96.6%, specificity of 100%, positive predictive value (PPV) of 100.0%, and negative predictive value (NPV) of 96.2% (Figure 1c). Principle components analysis (PCA) confirmed the segregation of melanomas from nevi based on the 40-CpG melanoma classifier (Figure 1d).

Despite the age difference between melanoma and nevus patients and age-associated CpGs being retained in the model, the 40-CpG melanoma classifier performed similarly in differentiating melanomas from nevi among both younger (≤ 50 years; AUC = 0.996) and older (> 50 years; AUC = 1.00) patients (Supplementary Figure S5 online). The classifier was also accurate irrespective of patient sex, tissue source, anatomic site, pigmentation, purity of the lesion, or degree of solar elastosis in adjacent skin (Supplementary Table S1 online). Compared with the dermatopathologist consensus, 2 of 89 samples (2.2%) were molecularly reclassified by the 40-CpG classifier; both were melanomas identified as nevi. One was a thin superficial spreading melanoma (Breslow thickness = 0.54 mm); the patient was alive with no evidence of disease (ANED) 15 months after diagnosis. The other was a nodular melanoma (Breslow thickness = 6.86 mm) from a 5-year old child who was ANED 33 months after diagnosis.

DAVID gene ontology analysis indicated that the 40-CpG melanoma classifier was enriched in homeobox genes that play roles in embryonic development and differentiation (e.g., *PAX3, TLX3, SHOX2, ALX3, SIX6, HOXD12, ONECUT1*), other transcriptional regulatory genes (*HAND2, TBX5, ZBTB38*), and genes involved in neurological processes (*NRXN1, SHANK3, HAND2, MBP, OPCML, SORCS2*) (Supplementary Table S2 online).

Validation of the classifier CpGs/genes in independent datasets

Data from published studies were used to confirm diagnostic methylation differences or to assess the biological relevance of differentially methylated genes by examining associated mRNA expression differences in melanomas versus nevi. As shown in the heatmap and associated waterfall plot in Figure 2a, application of the 40-CpG melanoma classifier to 105 primary melanomas in The Cancer Genome Atlas (TCGA) 450K methylation dataset (TCGA, 2015) confirmed 103 of these as melanomas despite TCGA primary melanomas being generally of higher tumor stage and obtained as frozen samples compared with UNC/UR study samples. Moreover, 367 metastatic melanomas from TCGA showed a similar range of classifier scores as the TCGA primary melanomas (Figure 2b). Using 450K methylation data from the study of Wouters et al. (Wouters et al., 2017), primary and metastatic melanomas were accurately distinguished from nevi with AUC of 1.000 (Figures 2c and 2d). Using 27K methylation data from the study of Gao and colleagues (Gao et al., 2013), PCA of methylation at 44 CpGs associated with genes in the 40-CpG diagnostic classifier distinguished primary melanomas from nevi (Figure 2e); only two of these probes directly overlapped probes in the 40-CpG classifier (cg03874199 in *HOXD12*; cg19352038 in *PAX3*) and these exhibited large differences in methylation between melanomas and nevi (Figure 2f). Differential mRNA expression of several diagnostic genes, including *PAX3*,

TBX5, *MBP*, *GOLIM4*, and *ANKH*, also differentiated primary melanomas from nevi in the dataset of Talantov *et al* (Talantov et al., 2005) (Supplementary Figure S6 online).

40-CpG melanoma classifier calls in uncertain samples

The 40-CpG classifier may be most clinically useful as an aid in the diagnosis of ambiguous melanocytic samples lacking agreement between dermatopathologists. Therefore, it was of interest to apply the 40-CpG melanoma classifier to the 41 diagnostically uncertain samples. The supervised heatmap in Figure 3a illustrates methylation levels at the 40 diagnostic CpGs in uncertain samples along with the melanomas and nevi having diagnostic consensus, ordered from lowest (negative for nevi) to highest classifier score (positive for melanoma). In total, 36 uncertain samples were called nevus and 5 were called melanoma by the classifier, as shown in the waterfall plot (Figure 3b). These results, together with the boxplots in Figure 3c summarizing classifier scores for the three diagnostic categories, show that the uncertain samples reside mainly among the nevi or between the nevi and primary invasive melanomas. This is further confirmed by PCA based on either the 40 classifier CpGs (Figure 3d) or the larger probe set (n=41,448) from which the classifier was derived (Supplementary Figure S7 online). The placement by the classifier of many diagnostically uncertain samples among the nevi is generally consistent with the pathology reviews in which 30 of 41 were called either nevus or uncertain by all the dermatopathology reviewers, while only 11 were called melanoma by any dermatopathology reviewer (Supplementary Table S8 online).

DISCUSSION

This study identified a 40-CpG melanoma classifier that distinguished cutaneous primary invasive melanomas, including thin melanomas, from nevi with a sensitivity of 96.6% and specificity of 100.0% in the validation set. Methylation analysis was successfully performed on >97% of FFPE samples. The classifier is comprised of a combination of CpGs exhibiting hypermethylation (n = 23) or hypomethylation (n = 17) in melanomas relative to nevi. Although melanoma patients are typically older than those being biopsied for nevi, as in this dataset, the diagnostic accuracy of the classifier was similarly very high among both younger and older patients. Importantly, the classifier confirmed as melanoma nearly all 472 primary and metastatic melanomas in TCGA and was further independently validated in published methylation and gene expression datasets. Application of the classifier to uncertain samples predicted many to be nevi and a few to be melanomas. Thus, we believe the identification of a diagnostically uncertain melanocytic specimen as melanoma by the classifier increases the probability that it is a melanoma. As expected, some classifier scores for uncertain samples fell near the interface of melanoma and nevus, suggesting they may be in transition toward melanoma, and future work will focus on the characterization of such samples.

The 40 classifier CpGs for melanoma are associated with 38 genes heavily enriched for homeobox developmental transcription factors (*ALX3*, *HOXD12*, *ONECUT1*, *PAX3*, *SHOX2*, *SIX6*, *TLX3*) and other transcriptional regulators (*TBX5*, *ZBTB38*, *MYT1L*). *PAX3*, a marker of melanocytic cells, is a key regulator of melanocyte development and has

putative roles in cell survival, migration, and differentiation (Dye et al., 2013; Medic and Ziman, 2009; 2010). Altered methylation of *PAX3* and several other melanoma classifier genes (*HOXD12*, *OPCML*, *GIMAP7*, *FAIM3*) has previously been reported in melanomas versus nevi (Conway et al., 2011; Furuta et al., 2004; Gao et al., 2013; Jin et al., 2015). *PROM1* (*CD133*), a stem cell marker involved in maintaining stem cell pluripotency, is frequently expressed in melanomas (Sharma et al., 2010; Zimmerer et al., 2016). Gene ontology analysis revealed associations of several diagnostic genes with neural tissues/processes (e.g., *OPCML*, *NRXN1*, *HAND2*, *MYT1L*, *MBP*, *TLX3*), reflecting their common embryologic derivation with melanocytes from neural crest cells (Noisa and Raivio, 2014). *FLJ22536*, recently identified as *CASC15*, is a putative mediator of neural growth and differentiation and a tumor suppressor in neuroblastoma (Russell et al., 2015), and in melanoma is linked to disease progression and phenotype switching between proliferative and invasive states (Lessard et al., 2015). Other diagnostic genes lack well-defined roles in melanoma; however, in other cancer types, a number exhibit aberrant expression (Gao et al., 2015; Jiang et al., 2008; Makiyama et al., 2005) and/or methylation (Jones et al., 2013; Kikuchi et al., 2013; Lai et al., 2008; Li et al., 2015; Semaan et al., 2016; Song et al., 2015; Wimmer et al., 2002; Yu et al., 2010; Zhao et al., 2013), function in apoptosis (Baras et al., 2009; Baras et al., 2011; Causeret et al., 2016) or differentiation (Zha et al., 2012), or are diagnostic (Semaan et al., 2016; Song et al., 2015; Xing et al., 2015), prognostic (Dietrich et al., 2013; Galluzzi et al., 2013; Qiu et al., 2015; Zheng et al., 2015; Zhou et al., 2014) or predictive biomarkers (Tada et al., 2011).

Our 40-CpG classifier for melanoma diagnosis may have advantages over other available approaches for melanoma diagnosis. In current clinical pathology practice, immunostains (e.g., Ki67, HMB45, p16) can aid pathologists' interpretation of melanocytic lesions, but single stains have low diagnostic accuracy (Uguen et al., 2015); combination staining may have higher accuracy but requires pathologist interpretation and lacks independent validation. Copy number analyses by comparative genomic hybridization (CGH) show that most melanomas, but few nevi, harbor numerous chromosomal changes (Bastian et al., 2000; Bauer and Bastian, 2006); however, CGH requires more tissue than is typically available from melanocytic samples. Fluorescence *in situ* hybridization detection of specific chromosomal changes is viewed directly on slides, using little tissue, but unlike CGH examines a limited number of chromosomes and requires technical expertise for interpretation (Busam, 2013). These currently utilized tests suffer from unclear diagnostic accuracy across the broad spectrum of melanoma and nevus subtypes (Ivan and Prieto, 2010) and limited independent validation. The Myriad MyPath Melanoma mRNA expression-based test showed reasonably high diagnostic accuracy (sensitivity and specificity >90%) for melanoma, but has a failure rate as high as 25% in FFPE archival samples (versus < 3% in this study) (Clarke et al., 2015; Ko et al., 2017). The 40-CpG melanoma classifier is an approach that combines high accuracy across diverse melanocytic subtypes, technical robustness, and the ability to reliably screen early, small melanomas.

A strength of this study is that the 40-CpG melanoma classifier was developed from a genome-wide methylation platform allowing unbiased selection of loci. Notably, some of the identified loci may function in the neoplastic transition toward melanoma. Further, we utilized melanomas with a wide range of different AJCC tumor stages, including thin T1a

melanomas, and diverse subtypes of both melanomas and nevi, such as dysplastic nevi, considered to be potential precursor lesions. For classification of melanoma or nevus in the training and validation sets, we required complete diagnostic consensus among three expert dermatopathologists and the original pathology report, crucial for achieving a highly accurate diagnostic classifier. Moreover, the classifier probes include only those with larger methylation differences between melanomas and nevi, which allows more reliable detection of these differences. Since the classifier was developed using FFPE samples similar to those typically found in clinical practice and requires amounts of DNA that can be recovered from most melanocytic samples, we expect the technology can be translated to clinical practice. Limitations of the study are its retrospective nature with potential sample selection bias. Another limitation is the absence of long-term follow-up of all patients.

In summary, our diagnostic 40-CpG melanoma classifier showed high accuracy in the validation set comprised of varied melanoma and nevus subtypes and was independently validated in public sample sets. Due to the robust nature of the assay, the 40-CpG melanoma classifier should be reliable on typical clinical samples. The assay also may have some advantages over other technologies due to its high diagnostic accuracy, need for less DNA, and robust methodology. However, additional studies are needed to further validate the performance of the classifier and optimize classifier score thresholds among larger numbers of samples, including rare melanocytic subtypes, especially in prospective studies with long-term follow-up.

MATERIALS AND METHODS

Patients and tissues

FFPE primary melanomas, nevi, and uncertain samples were assembled from the pathology archives of the University of North Carolina (UNC) Hospitals or from the University of Rochester (UR) Medical Center based on original diagnoses abstracted from pathology reports and diagnosed between 2001 and 2012. The Institutional Review Boards at UNC and the UR approved the study. Melanomas were chosen to span AJCC tumor stages and included common and less common subtypes (e.g., Spitzoid, nevoid, and desmoplastic melanomas). Nevi were chosen to include intradermal melanocytic nevi, including those with congenital pattern, compound melanocytic nevi with mild to severe dysplasia, Spitz and blue nevi, and other uncommon nevi (e.g. deep penetrating nevus, pigmented spindle cell nevus, and proliferative nodule in congenital pattern nevus). In addition, melanocytic proliferations of uncertain malignant potential were selected. Age, sex, race, and anatomic site were abstracted from the medical chart. Histopathological review of all samples was conducted independently by three expert dermatopathologists to assign diagnoses of melanoma or nevus or to identify uncertain samples. One dermatopathologist conducted a centralized histopathological review for histopathological pigment and adjacent solar elastosis of all the melanocytic lesions, for the histopathological subtype of nevi, and for histopathological subtype, Breslow thickness, mitoses, ulceration, and tumor infiltrating lymphocytes of the melanomas. Details of the histopathology are provided in Table 1. Details on the interobserver review are provided in the Supplementary Methods online. The

IRB determined the research met criteria for waiver of informed consent for research [45 CFR 46.116(d)] and waiver of HIPAA authorization [45 CFR 164.512(i)(2)(ii)].

DNA preparation and bisulfite treatment

Melanocytic lesions were manually microdissected using H&E slides as guides, and DNA was prepared as described (Thomas et al., 2004; Thomas et al., 2007). Sodium bisulfite modification of 250–300 ng DNA from each FFPE tissue was performed using the EZ DNA Methylation Lightning kit (Zymo Research, Orange, CA) according to the manufacturer's protocol.

Infinium HumanMethylation450 BeadChip analysis

Bisulfite-modified DNA (120 ng) was processed through the Illumina Infinium HD FFPE Restore protocol according to the manufacturer's instructions, and Illumina Infinium HumanMethylation450 BeadChip (450K) array analysis was performed in the Mammalian Genotyping Core at UNC. Details on methylation array analysis and data preprocessing are provided in the Supplementary Methods online. The final dataset contained 383,229 probes and 203 samples (89 melanomas, 73 nevi, 41 uncertain, and 12 controls). Methylation data were deposited to Gene Expression Omnibus under accession number GSE120878.

Statistical analyses

To develop a diagnostic classifier distinguishing melanomas from nevi, melanomas and nevi with diagnostic consensus were split into training (67% of each sample class) and validation (the remaining 33%) sets. Multiple predictive models based on different probe sets were tested for their ability to distinguish melanomas from nevi; these included accounting for effects of age and limiting probes to the most differentially methylated. For each probe set, Monte-Carlo cross validation with 100 iterations was performed on training samples using the ElasticNet algorithm implemented in R package glmnet (Zou and Hastie, 2005) to obtain optimal parameters (alpha and the number of probes) that best differentiate melanomas. In each iteration, 2/3 of the training set was randomly selected to build the elastic model and to predict on the rest of the 1/3 in the training set. Based on the average AUC across 100 iterations, we determined the number of probes to be included in the final model. Classifier scores were calculated using the β value of selected probes in the final model. Heatmaps were generated to illustrate methylation at the diagnostic probe set, and PCA was performed to illustrate the segregation of melanomas and nevi. Additional details of model development and validation are provided in the Supplementary Methods online.

Independent validation in published methylation datasets

Illumina 450K methylation data for TCGA melanomas were downloaded from the Broad Institute Firehose web portal (http://firebrowse.org/) (version 2016012800). Illumina 450K methylation data for melanomas and nevi from the study of Wouters et al (Wouters et al., 2017) were obtained from Gene Expression Omnibus (GEO) (accession number GSE86355). Illumina Infinium HumanMethylation27 (27K) methylation data for melanomas and nevi were downloaded from GEO (accession number GSE45266) from the

study of Gao *et al* (Gao et al., 2013). Details of independent validation are provided in the Supplementary Methods online.

Supplementary Material

Refer to Web version on PubMed Central for supplementary material.

Acknowledgements:

We thank the staff of the Mammalian Genotyping Core at UNC for performing the methylation assays.

Funding: This work was funded by National Cancer Institute grants R21CA134368, R33CA160138, and R03CA199487 to K Conway and NE Thomas, P01CA206980 to NE Thomas, and P30CA016086 to HS Earp. The LCCC Mammalian Genotyping Core Facility performed the methylation assays and was supported in part by a grant from the National Institute of Environmental Health Sciences (P30ES010126). This work was also supported by the LCCC Bioinformatics Core and University Cancer Research Fund support to S Moschos.

Abbreviations:

AUC	area under the curve
FFPE	formalin-fixed, paraffin-embedded
IQR	interquartile range
NPV	negative predictive value
PA	promoter-associated
PCA	principal component analysis
PPV	positive predictive value
ROC	receiver operating characteristic
TCGA	The Cancer Genome Atlas
TSS	transcription start site
UCTS	unclassified cell type-specific
UNC	University of North Carolina
uncl	unclassified
UR	University of Rochester
UTR	untranslated region

REFERENCES

Alexandrescu DT, Kauffman CL, Jatkoe TA, Hartmann DP, Vener T, Wang H, et al. Melanoma-specific marker expression in skin biopsy tissues as a tool to facilitate melanoma diagnosis. J Invest Dermatol 2010;130(7):1887–92. [PubMed: 20357814]

Andtbacka RH, Kaufman HL, Collichio F, Amatruda T, Senzer N, Chesney J, et al. Talimogene Laherparepvec Improves Durable Response Rate in Patients With Advanced Melanoma. J Clin Oncol 2015;33(25):2780–8. [PubMed: 26014293]

Arai E, Kanai Y. DNA methylation profiles in precancerous tissue and cancers: carcinogenetic risk estimation and prognostication based on DNA methylation status. Epigenomics 2010;2(3):467–81. [PubMed: 22121905]

Balch CM, Gershenwald JE, Soong SJ, Thompson JF, Atkins MB, Byrd DR, et al. Final version of 2009 AJCC melanoma staging and classification. J Clin Oncol 2009;27(36):6199–206. [PubMed: 19917835]

Baras A, Yu Y, Filtz M, Kim B, Moskaluk CA. Combined genomic and gene expression microarray profiling identifies ECOP as an upregulated gene in squamous cell carcinomas independent of DNA amplification. Oncogene 2009;28(32):2919–24. [PubMed: 19525979]

Baras AS, Solomon A, Davidson R, Moskaluk CA. Loss of VOPP1 overexpression in squamous carcinoma cells induces apoptosis through oxidative cellular injury. Lab Invest 2011;91(8):1170–80. [PubMed: 21519330]

Bastian BC, LeBoit PE, Pinkel D. Mutations and copy number increase of HRAS in Spitz nevi with distinctive histopathological features. Am J Pathol 2000;157(3):967–72. [PubMed: 10980135]

Bastian BC, Olshen AB, LeBoit PE, Pinkel D. Classifying melanocytic tumors based on DNA copy number changes. Am J Pathol 2003;163(5):1765–70. [PubMed: 14578177]

Bauer J, Bastian BC. Distinguishing melanocytic nevi from melanoma by DNA copy number changes: comparative genomic hybridization as a research and diagnostic tool. Dermatol Ther 2006;19(1): 40–9. [PubMed: 16405569]

Brochez L, Verhaeghe E, Grosshans E, Haneke E, Pierard G, Ruiter D, et al. Inter-observer variation in the histopathological diagnosis of clinically suspicious pigmented skin lesions. J Pathol 2002;196(4):459–66. [PubMed: 11920743]

Busam KJ. Molecular pathology of melanocytic tumors. Semin Diagn Pathol 2013;30(4):362–74. [PubMed: 24342290]

Causeret F, Sumia I, Pierani A. Kremen1 and Dickkopf1 control cell survival in a Wnt-independent manner. Cell Death Differ 2016;23(2):323–32. [PubMed: 26206087]

Clarke JM, George DJ, Lisi S, Salama AKS. Immune Checkpoint Blockade: The New Frontier in Cancer Treatment. Target Oncol 2018.

Clarke LE, Warf MB, Flake DD 2nd, Hartman AR, Tahan S, Shea CR, et al. Clinical validation of a gene expression signature that differentiates benign nevi from malignant melanoma. J Cutan Pathol 2015;42(4):244–52. [PubMed: 25727210]

Conway K, Edmiston SN, Khondker ZS, Groben PA, Zhou X, Chu H, et al. DNA-methylation profiling distinguishes malignant melanomas from benign nevi. Pigment Cell Melanoma Res 2011;24(2):352–60. [PubMed: 21375697]

Dietrich D, Jung M, Puetzer S, Leisse A, Holmes EE, Meller S, et al. Diagnostic and prognostic value of SHOX2 and SEPT9 DNA methylation and cytology in benign, paramalignant and malignant pleural effusions. PLoS One 2013;8(12):e84225. [PubMed: 24386354]

Dye DE, Medic S, Ziman M, Coombe DR. Melanoma biomolecules: independently identified but functionally intertwined. Front Oncol 2013;3:252. [PubMed: 24069584]

Elmore J, Barnhill R, Elder D, Longton G, Pepe M, Reisch L, et al. Pathologists' diagnosis of invasive melanoma and melanocytic proliferations: observer accuracy and resproducibility study. BMJ 2017;357:j2813. [PubMed: 28659278]

Farmer ER, Gonin R, Hanna MP. Discordance in the histopathologic diagnosis of melanoma and melanocytic nevi between expert pathologists. Hum Pathol 1996;27(6):528–31. [PubMed: 8666360]

Fung MA. Terminology and management of dysplastic nevi: responses from 145 dermatologists. Arch Dermatol 2003;139(10):1374–5. [PubMed: 14568850]

Furuta J, Umebayashi Y, Miyamoto K, Kikuchi K, Otsuka F, Sugimura T, et al. Promoter methylation profiling of 30 genes in human malignant melanoma. Cancer Sci 2004;95(12):962–8. [PubMed: 15596045]

Galluzzi L, Goubar A, Olaussen KA, Vitale I, Senovilla L, Michels J, et al. Prognostic value of LIPC in non-small cell lung carcinoma. Cell Cycle 2013;12(4):647–54. [PubMed: 23343765]

Gao C, Pang M, Zhou Z, Long S, Dong D, Yang J, et al. Epidermal growth factor receptor-coamplified and overexpressed protein (VOPP1) is a putative oncogene in gastric cancer. Clin Exp Med 2015;15(4):469–75. [PubMed: 25398664]

Gao L, Smit MA, van den Oord JJ, Goeman JJ, Verdegaal EM, van der Burg SH, et al. Genome-wide promoter methylation analysis identifies epigenetic silencing of MAPK13 in primary cutaneous melanoma. Pigment Cell Melanoma Res 2013;26(4):542–54. [PubMed: 23590314]

Gao L, van den Hurk K, Moerkerk PT, Goeman JJ, Beck S, Gruis NA, et al. Promoter CpG island hypermethylation in dysplastic nevus and melanoma: CLDN11 as an epigenetic biomarker for malignancy. J Invest Dermatol 2014;134(12):2957–66. [PubMed: 24999589]

Gerami P, Busam K, Cochran A, Cook MG, Duncan LM, Elder DE, et al. Histomorphologic assessment and interobserver diagnostic reproducibility of atypical spitzoid melanocytic neoplasms with long-term follow-up. Am J Surg Pathol 2014;38(7):934–40. [PubMed: 24618612]

Gerami P, Jewell SS, Morrison LE, Blondin B, Schulz J, Ruffalo T, et al. Fluorescence in situ hybridization (FISH) as an ancillary diagnostic tool in the diagnosis of melanoma. Am J Surg Pathol 2009;33(8):1146–56. [PubMed: 19561450]

Haqq C, Nosrati M, Sudilovsky D, Crothers J, Khodabakhsh D, Pulliam BL, et al. The gene expression signatures of melanoma progression. Proc Natl Acad Sci U S A 2005;102(17):6092–7. [PubMed: 15833814]

Herman JG, Baylin SB. Gene silencing in cancer in association with promoter hypermethylation. N Engl J Med 2003;349(21):2042–54. [PubMed: 14627790]

Hodi FS, Chesney J, Pavlick AC, Robert C, Grossmann KF, McDermott DF, et al. Combined nivolumab and ipilimumab versus ipilimumab alone in patients with advanced melanoma: 2-year overall survival outcomes in a multicentre, randomised, controlled, phase 2 trial. Lancet Oncol 2016;17(11):1558–68. [PubMed: 27622997]

Hoon DS, Spugnardi M, Kuo C, Huang SK, Morton DL, Taback B. Profiling epigenetic inactivation of tumor suppressor genes in tumors and plasma from cutaneous melanoma patients. Oncogene 2004;23(22):4014–22. [PubMed: 15064737]

Ivan D, Prieto VG. Use of immunohistochemistry in the diagnosis of melanocytic lesions: applications and pitfalls. Future Oncol 2010;6(7):1163–75. [PubMed: 20624128]

Jiang X, Zhang W, Kayed H, Zheng P, Giese NA, Friess H, et al. Loss of ONECUT1 expression in human pancreatic cancer cells. Oncol Rep 2008;19(1):157–63. [PubMed: 18097590]

Jin SG, Xiong W, Wu X, Yang L, Pfeifer GP. The DNA methylation landscape of human melanoma. Genomics 2015;106(6):322–30. [PubMed: 26384656]

Jones A, Teschendorff AE, Li Q, Hayward JD, Kannan A, Mould T, et al. Role of DNA methylation and epigenetic silencing of HAND2 in endometrial cancer development. PLoS Med 2013;10(11):e1001551. [PubMed: 24265601]

Kikuchi Y, Tsuji E, Yagi K, Matsusaka K, Tsuji S, Kurebayashi J, et al. Aberrantly methylated genes in human papillary thyroid cancer and their association with BRAF/RAS mutation. Front Genet 2013;4:271. [PubMed: 24367375]

Ko JS, Matharoo-Ball B, Billings SD, Thomson BJ, Tang JY, Sarin KY, et al. Diagnostic Distinction of Malignant Melanoma and Benign Nevi by a Gene Expression Signature and Correlation to Clinical Outcomes. Cancer Epidemiol Biomarkers Prev 2017;26(7):1107–13. [PubMed: 28377414]

Koh SS, Opel ML, Wei JP, Yau K, Shah R, Gorre ME, et al. Molecular classification of melanomas and nevi using gene expression microarray signatures and formalin-fixed and paraffin-embedded tissue. Mod Pathol 2009;22(4):538–46. [PubMed: 19270649]

Lai HC, Lin YW, Huang TH, Yan P, Huang RL, Wang HC, et al. Identification of novel DNA methylation markers in cervical cancer. Int J Cancer 2008;123(1):161–7. [PubMed: 18398837]

Landow SM, Gjelsvik A, Weinstock MA. Mortality burden and prognosis of thin melanomas overall and by subcategory of thickness, SEER registry data, 1992–2013. J Am Acad Dermatol 2017;76(2):258–63. [PubMed: 27887797]

Lessard L, Liu M, Marzese DM, Wang H, Chong K, Kawas N, et al. The CASC15 Long Intergenic Noncoding RNA Locus Is Involved in Melanoma Progression and Phenotype Switching. J Invest Dermatol 2015;135(10):2464–74. [PubMed: 26016895]

Li C, Tang L, Zhao L, Li L, Xiao Q, Luo X, et al. OPCML is frequently methylated in human colorectal cancer and its restored expression reverses EMT via downregulation of smad signaling. Am J Cancer Res 2015;5(5):1635–48. [PubMed: 26175934]

Long GV, Flaherty KT, Stroyakovskiy D, Gogas H, Levchenko E, de Braud F, et al. Dabrafenib plus trametinib versus dabrafenib monotherapy in patients with metastatic BRAF V600E/K-mutant melanoma: long-term survival and safety analysis of a phase 3 study. Ann Oncol 2017;28(7):1631–9. [PubMed: 28475671]

Makiyama K, Hamada J, Takada M, Murakawa K, Takahashi Y, Tada M, et al. Aberrant expression of HOX genes in human invasive breast carcinoma. Oncol Rep 2005;13(4):673–9. [PubMed: 15756441]

Medic S, Ziman M. PAX3 across the spectrum: from melanoblast to melanoma. Crit Rev Biochem Mol Biol 2009;44(2–3):85–97. [PubMed: 19401874]

Medic S, Ziman M. PAX3 expression in normal skin melanocytes and melanocytic lesions (naevi and melanomas). PLoS One 2010;5(4):e9977. [PubMed: 20421967]

Noisa P, Raivio T. Neural crest cells: from developmental biology to clinical interventions. Birth Defects Res C Embryo Today 2014;102(3):263–74. [PubMed: 25226872]

North JP, Garrido MC, Kolaitis NA, LeBoit PE, McCalmont TH, Bastian BC. Fluorescence in situ hybridization as an ancillary tool in the diagnosis of ambiguous melanocytic neoplasms: a review of 804 cases. Am J Surg Pathol 2014;38(6):824–31. [PubMed: 24618603]

Plass C Cancer epigenomics. Hum Mol Genet 2002;11(20):2479–88. [PubMed: 12351584]

Qiu ZX, Zhao S, Mo XM, Li WM. Overexpression of PROM1 (CD133) confers poor prognosis in non-small cell lung cancer. Int J Clin Exp Pathol 2015;8(6):6589–95. [PubMed: 26261540]

Ribas A, Hamid O, Daud A, Hodi FS, Wolchok JD, Kefford R, et al. Association of Pembrolizumab With Tumor Response and Survival Among Patients With Advanced Melanoma. JAMA 2016;315(15):1600–9. [PubMed: 27092830]

Ribas A, Puzanov I, Dummer R, Schadendorf D, Hamid O, Robert C, et al. Pembrolizumab versus investigator-choice chemotherapy for ipilimumab-refractory melanoma (KEYNOTE-002): a randomised, controlled, phase 2 trial. Lancet Oncol 2015;16(8):908–18. [PubMed: 26115796]

Robert C, Long GV, Brady B, Dutriaux C, Maio M, Mortier L, et al. Nivolumab in previously untreated melanoma without BRAF mutation. N Engl J Med 2015;372(4):320–30. [PubMed: 25399552]

Russell MR, Penikis A, Oldridge DA, Alvarez-Dominguez JR, McDaniel L, Diamond M, et al. CASC15-S Is a Tumor Suppressor lncRNA at the 6p22 Neuroblastoma Susceptibility Locus. Cancer Res 2015;75(15):3155–66. [PubMed: 26100672]

Schachter J, Ribas A, Long GV, Arance A, Grob JJ, Mortier L, et al. Pembrolizumab versus ipilimumab for advanced melanoma: final overall survival results of a multicentre, randomised, open-label phase 3 study (KEYNOTE-006). Lancet 2017;390(10105):1853–62. [PubMed: 28822576]

Semaan A, van Ellen A, Meller S, Bergheim D, Branchi V, Lingohr P, et al. SEPT9 and SHOX2 DNA methylation status and its utility in the diagnosis of colonic adenomas and colorectal adenocarcinomas. Clin Epigenetics 2016;8:100. [PubMed: 27660666]

Shaikh WR, Dusza SW, Weinstock MA, Oliveria SA, Geller AC, Halpern AC. Melanoma Thickness and Survival Trends in the United States, 1989 to 2009. J Natl Cancer Inst 2016;108(1).

Shain AH, Yeh I, Kovalyshyn I, Sriharan A, Talevich E, Gagnon A, et al. The Genetic Evolution of Melanoma from Precursor Lesions. N Engl J Med 2015;373(20):1926–36. [PubMed: 26559571]

Sharma BK, Manglik V, Elias EG. Immuno-expression of human melanoma stem cell markers in tissues at different stages of the disease. J Surg Res 2010;163(1):e11–5. [PubMed: 20638684]

Shoo BA, Sagebiel RW, Kashani-Sabet M. Discordance in the histopathologic diagnosis of melanoma at a melanoma referral center. J Am Acad Dermatol 2010;62(5):751–6. [PubMed: 20303612]

Siegel RL, Miller KD, Jemal A. Cancer statistics, 2018. CA Cancer J Clin 2018;68(1):7–30. [PubMed: 29313949]

Song L, Yu H, Li Y. Diagnosis of Lung Cancer by SHOX2 Gene Methylation Assay. Mol Diagn Ther 2015;19(3):159–67. [PubMed: 26014676]

Strauss RM, Elliott F, Affleck P, Boon AP, Newton-Bishop JA. A retrospective study addressed to understanding what predicts severe histological dysplasia/early melanoma in excised atypical melanocytic lesions. Br J Dermatol 2007;157(4):758–64. [PubMed: 17714559]

Tada Y, Yokomizo A, Shiota M, Tsunoda T, Plass C, Naito S. Aberrant DNA methylation of T-cell leukemia, homeobox 3 modulates cisplatin sensitivity in bladder cancer. Int J Oncol 2011;39(3): 727–33. [PubMed: 21617853]

Talantov D, Mazumder A, Yu JX, Briggs T, Jiang Y, Backus J, et al. Novel genes associated with malignant melanoma but not benign melanocytic lesions. Clin Cancer Res 2005;11(20):7234–42. [PubMed: 16243793]

TCGA N Genomic Classification of Cutaneous Melanoma. Cell 2015;161(7):1681–96. [PubMed: 26091043]

Thomas NE, Alexander A, Edmiston SN, Parrish E, Millikan RC, Berwick M, et al. Tandem BRAF mutations in primary invasive melanomas. J Invest Dermatol 2004;122(5):1245–50. [PubMed: 15140228]

Thomas NE, Edmiston SN, Alexander A, Millikan RC, Groben PA, Hao H, et al. Number of nevi and early-life ambient UV exposure are associated with BRAF-mutant melanoma. Cancer Epidemiol Biomarkers Prev 2007;16(5):991–7. [PubMed: 17507627]

Thomas NE, Slater NA, Edmiston SN, Zhou X, Kuan PF, Groben PA, et al. DNA methylation profiles in primary cutaneous melanomas are associated with clinically significant pathologic features. Pigment Cell Melanoma Res 2014;27(6):1097–105. [PubMed: 24986547]

Uguen A, Talagas M, Costa S, Duigou S, Bouvier S, De Braekeleer M, et al. A p16-Ki-67-HMB45 immunohistochemistry scoring system as an ancillary diagnostic tool in the diagnosis of melanoma. Diagn Pathol 2015;10:195. [PubMed: 26503349]

Veenhuizen KC, De Wit PE, Mooi WJ, Scheffer E, Verbeek AL, Ruiter DJ. Quality assessment by expert opinion in melanoma pathology: experience of the pathology panel of the Dutch Melanoma Working Party. J Pathol 1997;182(3):266–72. [PubMed: 9349228]

Whiteman DC, Baade PD, Olsen CM. More people die from thin melanomas (1 mm) than from thick melanomas (>4 mm) in Queensland, Australia. J Invest Dermatol 2015;135(4):1190–3. [PubMed: 25330295]

Wimmer K, Zhu Xx XX, Rouillard JM, Ambros PF, Lamb BJ, Kuick R, et al. Combined restriction landmark genomic scanning and virtual genome scans identify a novel human homeobox gene, ALX3, that is hypermethylated in neuroblastoma. Genes Chromosomes Cancer 2002;33(3):285–94. [PubMed: 11807986]

Wouters J, Vizoso M, Martinez-Cardus A, Carmona FJ, Govaere O, Laguna T, et al. Comprehensive DNA methylation study identifies novel progression-related and prognostic markers for cutaneous melanoma. Bmc Med 2017;15(1):101. [PubMed: 28578692]

Xing BL, Li T, Tang ZH, Jiao L, Ge SM, Qiang X, et al. Cumulative methylation alternations of gene promoters and protein markers for diagnosis of epithelial ovarian cancer. Genet Mol Res 2015;14(2):4532–40. [PubMed: 25966226]

Yu J, Ma X, Cheung KF, Li X, Tian L, Wang S, et al. Epigenetic inactivation of T-box transcription factor 5, a novel tumor suppressor gene, is associated with colon cancer. Oncogene 2010;29(49): 6464–74. [PubMed: 20802524]

Zha Y, Ding E, Yang L, Mao L, Wang X, McCarthy BA, et al. Functional dissection of HOXD cluster genes in regulation of neuroblastoma cell proliferation and differentiation. PLoS One 2012;7(8):e40728. [PubMed: 22879880]

Zhao Y, Zhou H, Ma K, Sun J, Feng X, Geng J, et al. Abnormal methylation of seven genes and their associations with clinical characteristics in early stage non-small cell lung cancer. Oncol Lett 2013;5(4):1211–8. [PubMed: 23599765]

Zheng Y, Li YF, Wang W, Chen YM, Wang DD, Zhao JJ, et al. High expression level of T-box transcription factor 5 predicts unfavorable survival in stage I and II gastric adenocarcinoma. Oncol Lett 2015;10(4):2021–6. [PubMed: 26622790]

Zhou F, Tao G, Chen X, Xie W, Liu M, Cao X. Methylation of OPCML promoter in ovarian cancer tissues predicts poor patient survival. Clin Chem Lab Med 2014;52(5):735–42. [PubMed: 24327526]

Zimmerer RM, Matthiesen P, Kreher F, Kampmann A, Spalthoff S, Jehn P, et al. Putative CD133+ melanoma cancer stem cells induce initial angiogenesis in vivo. Microvasc Res 2016;104:46–54. [PubMed: 26656667]

Zou H, Hastie T. Regularization and variable selection via the Elastic Net. Journal of the Royal Statistical Society 2005;Series B (Statistical Methodology)(67):301–20.

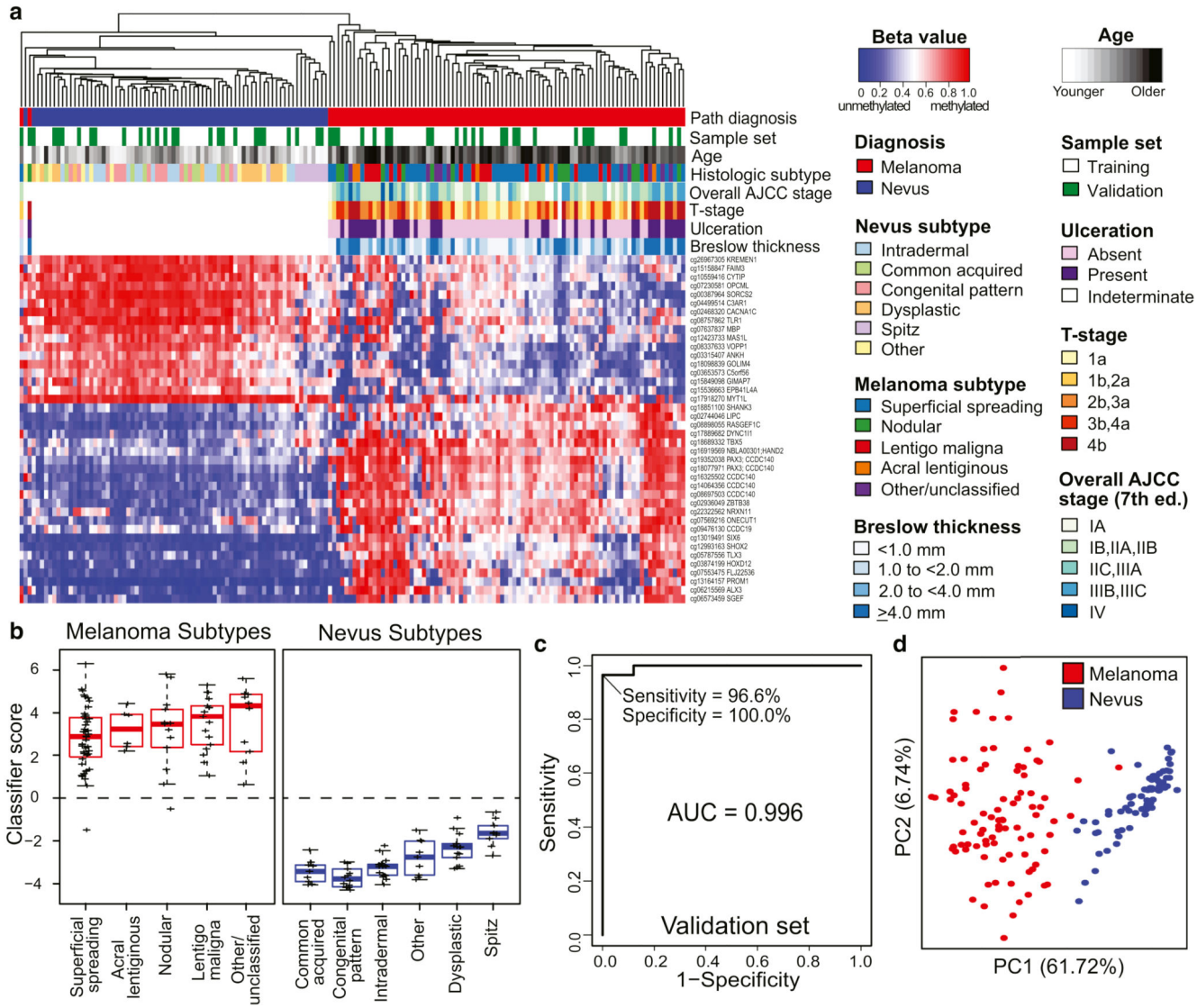

Figure 1. Performance of the 40-CpG melanoma classifier in training and/or validation sets.

Specimens in the training (60 melanomas and 48 nevi) and validation (29 melanomas and 25 nevi) sets had diagnostic consensus on interobserver review. The 40 diagnostic probes were identified from the model that analyzed annotated probes with IQR > 0.2 β between melanomas and nevi. (a) Heatmap showing methylation at 40 classifier probes in melanomas (red) and nevi (blue) from the combined training (white) and validation sets (green). Red represents highly methylated and blue represents unmethylated. (b) Boxplots of classifier scores for histological subtypes of nevi and melanomas. (c) ROC plot showing diagnostic accuracy in the validation set. (d) PCA showing the segregation of melanoma and nevus samples based on the 40 CpG classifier.

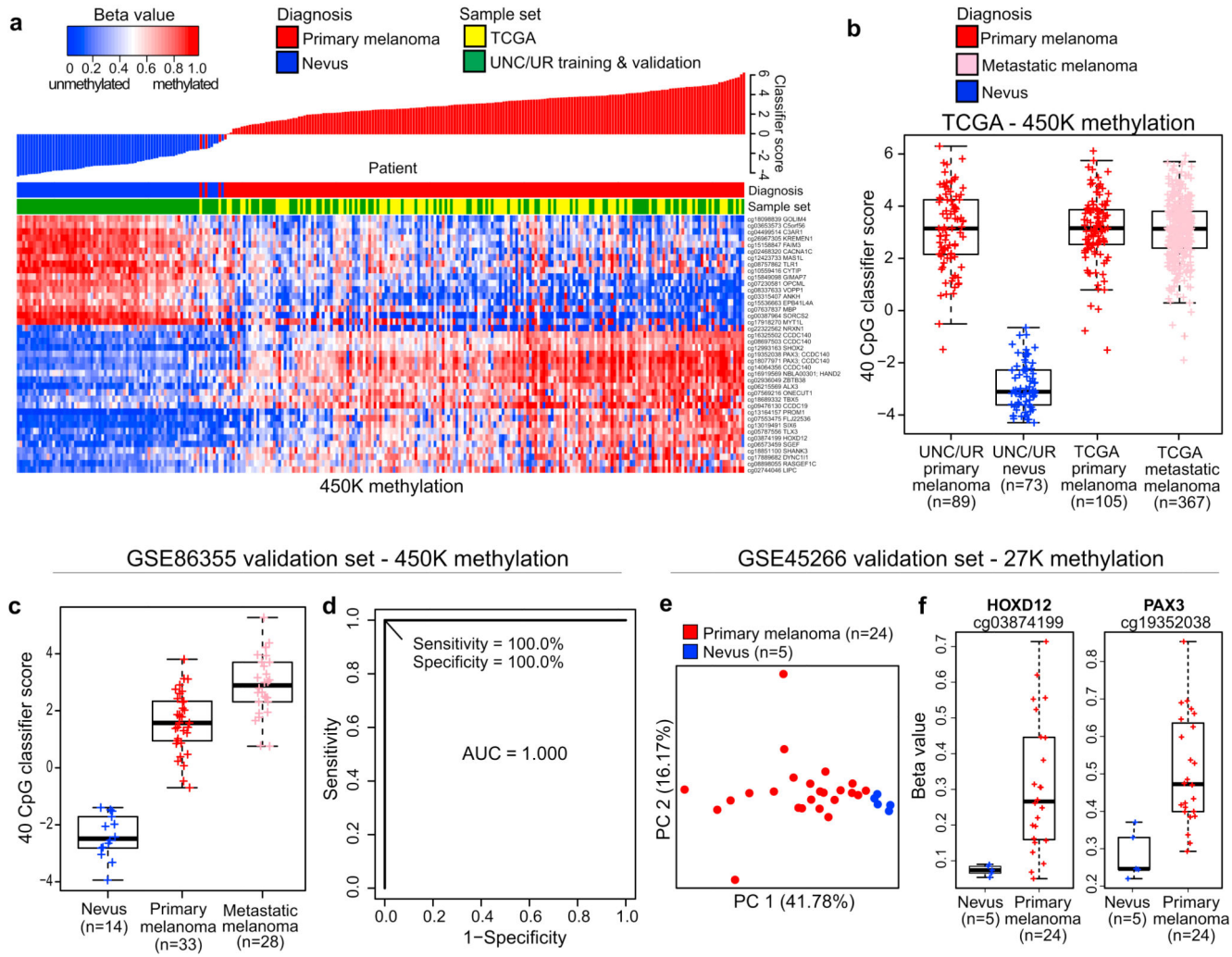

Figure 2. Independent validation of differential methylation at classifier CpG loci.

Validation of the diagnostic classifier was conducted in three public datasets. (a) 40-CpG methylation heatmap and waterfall plot of classifier scores in 105 primary melanomas from TCGA (TCGA, 2015) (yellow) compared with 89 melanomas and 73 nevi from UNC/UR (green). (b) Boxplots showing classifier scores for TCGA primary or metastatic melanomas and UNC/UR primary melanomas and nevi. (c) Boxplots showing classifier scores for 33 primary and 28 metastatic melanomas, and 14 nevi, and (d) ROC plot showing the diagnostic accuracy of the 40 CpG classifier comparing nevi to primary melanomas in the GSE86355 450K methylation dataset. In the GSE45266 27K methylation dataset, (e) PCA of methylation at 44 CpGs associated with diagnostic classifier genes illustrates segregation of 24 primary melanomas from 5 nevi, and (f) boxplots showing methylation differences at the 2 CpG loci (cg3874199 and cg19352038) directly matching 450K probes in the diagnostic classifier.

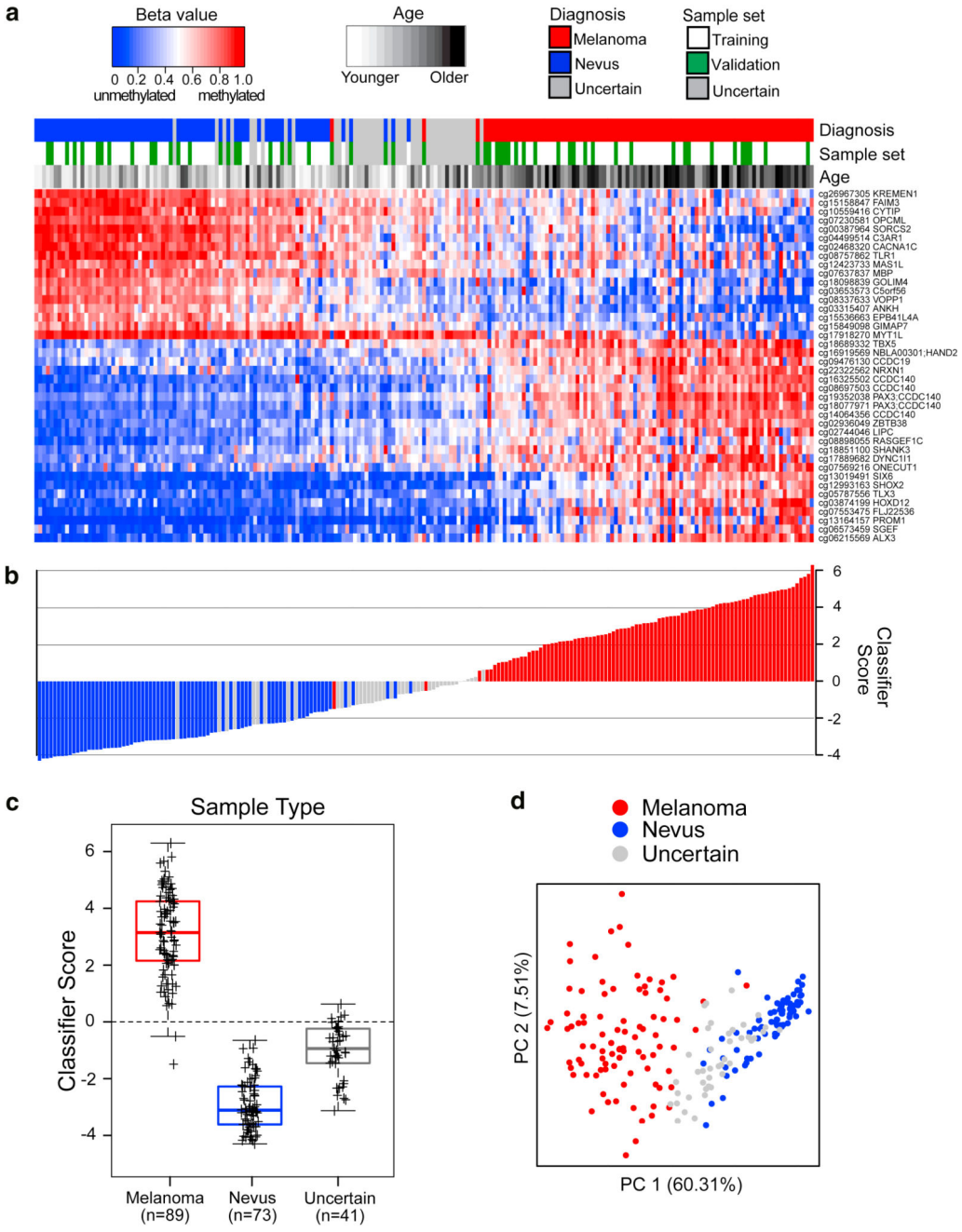

Figure 3. Diagnostic 40-CpG melanoma classifier calls on melanomas, nevi, and diagnostically uncertain samples.

Interobserver dermatopathologic review identified 89 melanomas, 73 nevi, and 41 uncertain samples. (a) Supervised heatmap, ordered left to right from lowest to highest diagnostic classifier score, showing methylation levels at the 40 diagnostic CpGs in melanomas (red) or nevi (blue) from the training (white) or validation sets (green), or uncertain samples (gray). (b) Waterfall plot of classifier scores, ordered as in the heatmap, and color-coded for diagnosis. (c) Boxplots of classifier scores for each diagnostic category, with median and interquartile range encompassed by each box. The broken lines indicate the classifier score

threshold for distinguishing melanomas from nevi. (d) PCA plot shows sample segregation based on the 40 CpG classifier.

Table 1.

Clinical and histopathological characteristics of cutaneous melanocytic nevi, primary melanomas, and melanocytic proliferations of uncertain malignant potential evaluated using 450K Illumina Infinium DNA methylation arrays

	Training Set		Validation Set		Validation vs Training		Melanocytic Proliferations of Uncertain Malignant Potential[2] (n = 41)
	Nevi (n = 48)	Primary Melanomas (n = 60)	Nevi (n = 25)	Primary Melanomas (n = 29)	Nevi	Primary Melanomas	
Characteristic	No (%)	No (%)	No (%)	No (%)	*P*[1]	*P*[1]	No (%)
Laboratory processing of unstained FFPE tissue sections							
University of North Carolina pathology archives	45 (94)	56 (93)	22 (88)	28 (97)	.41	1.00	41 (100)
University of Rochester pathology archives	3 (6)	4 (7)	3 (12)	1 (3)			–
Sex							
Male	23 (48)	38 (63)	12 (48)	19 (66)	1.00	1.00	16 (39)
Female	25 (52)	22 (37)	13 (52)	10 (34)			25 (61)
Age at diagnosis of mole or primary melanoma							
≤ 50 years	40 (83)	13 (22)	22 (88)	8 (28)	.74	.60	30 (73)
> 50 years	8 (17)	47 (78)	3 (12)	21 (72)			11 (27)
Race							
White of European origin	35 (73)	52 (87)	16 (64)	27 (93)	.42	.41	24 (59)
Other	4 (8)	1 (2)	1 (4)	1 (3)			7 (17)
Unknown	9 (19)	7 (12)	8 (32)	1 (3)			10 (24)
Anatomic site of mole or primary melanoma							
Head/neck	11 (23)	20 (33)	8 (32)	9 (31)	.46	1.00	4 (10)
Trunk	25 (52)	18 (30)	12 (48)	9 (31)			23 (56)
Upper extremities	5 (10)	11 (18)	4 (16)	6 (21)			3 (7)
Lower extremities	7 (15)	11 (18)	1 (4)	5 (17)			11 (27)
Histopathological subtype of primary melanoma							
Superficial Spreading	–	27 (45)	–	16 (55)		.93	–
Nodular	–	9 (15)	–	4 (14)			–

Characteristic	Training Set		Validation Set		Validation vs Training		Melanocytic Proliferations of Uncertain Malignant Potential[2] (n = 41)
	Nevi (n = 48)	Primary Melanomas (n = 60)	Nevi (n = 25)	Primary Melanomas (n = 29)	Nevi	Primary Melanomas	
	No (%)	No (%)	No (%)	No (%)	*P*[1]	*P*[1]	No (%)
Lentigo maligna	–	12 (20)	–	5 (17)			–
Acral lentiginous	–	5 (8)	–	1 (3)			–
Other/unclassified[3]	–	7 (12)	–	3 (10)			–
Melanocytic nevus type							
Intradermal	10 (21)	–	7 (28)	–	.62		–
Common acquired	8 (17)	–	1 (4)	–			–
Congenital pattern	8 (17)	–	6 (24)	–			–
Dysplastic	9 (19)	–	5 (20)	–			–
Spitz	6 (13)	–	4 (16)	–			–
Other[4]	7 (15)	–	2 (8)	–			–
Breslow thickness of primary melanoma, mm							
Median (range)	–	2.30 (0.48–17.00)	–	1.40 (0.37–11.00)		.17	–
0.01 to 1.00	–	9 (15)	–	11 (38)		.14	–
1.01 to 2.00	–	20 (33)	–	7 (24)			–
2.01 to 4.00	–	13 (22)	–	4 (14)			–
>4.00	–	18 (30)	–	7 (24)			–
Ulceration of primary melanoma							
Absent	–	33 (55)	–	20 (69)		.50	–
Present	–	26 (43)	–	9 (31)			–
Indeterminate	–	1 (2)	–	0			–
Mitoses of primary melanoma							
Absent	–	9 (15)	–	8 (28)		.25	–
Present	–	51 (85)	–	21 (72)			–
7th edition (2009) AJCC tumor stage at diagnosis							
T1a	–	8 (13)	–	6 (21)		.36	–
T1b/T2a	–	14 (23)	–	11 (38)			–

Characteristic	Training Set		Validation Set		Validation vs Training		Melanocytic Proliferations of Uncertain Malignant Potential[2] (n = 41)
	Nevi (n = 48)	Primary Melanomas (n = 60)	Nevi (n = 25)	Primary Melanomas (n = 29)	Nevi	Primary Melanomas	
	No (%)	No (%)	No (%)	No (%)	*P*[1]	*P*[1]	No (%)
T2b/T3a	–	13 (22)	–	4 (14)			–
T3b/T4a	–	12 (20)	–	2 (7)			–
T4b	–	12 (20)	–	6 (21)			–
Indeterminate	–	1 (2)	–	0			–
Tumor infiltrating lymphocyte grade of primary melanoma							
Absent	–	17 (28)	–	4 (14)		.43	–
Non-brisk	–	29 (48)	–	17 (59)			–
Brisk	–	13 (22)	–	8 (28)			–
Indeterminate	–	1 (2)	–	0			–
Pigment of the melanocytic lesion							
Absent	9 (19)	14 (23)	4 (16)	3 (10)	.37	.10	8 (20)
Medium	27 (56)	31 (52)	18 (72)	22 (76)			22 (54)
Heavy	12 (25)	15 (25)	3 (12)	4 (14)			11 (27)
Solar Elastosis adjacent to the melanocytic lesion							
Absent	27 (56)	14 (23)	17 (68)	8 (28)	.79	.30	35 (85)
Mild to moderate	4 (8)	26 (43)	2 (8)	16 (55)			4 (10)
Severe	2 (4)	14 (23)	1 (4)	5 (17)			1 (2)
Indeterminate	15 (31)	6 (10)	5 (20)	0			1 (2)

[1] *P*-values were derived from the Fisher's exact test except the Wilcoxon rank-sum test was used to compare the median Breslow thickness between the validation and training sets.

[2] Melanocytic proliferations were considered uncertain if there was interobserver disagreement between any of 3 dermatopathology readers or the pathology report diagnosis of nevus vs. melanoma or one of the dermatopathologists or pathology report described the specimen as having uncertain diagnosis.

[3] Other types of melanoma include nevoid (n = 2), desmoplastic (n = 1), spindle cell (n = 1), Spitzoid (n = 1), unclassified (n = 5).

[4] Other includes cellular blue nevus (n = 2), combined intradermal or sclerotic blue nevus, not cellular (n = 1), combined nevus with compound congenital pattern and deep penetrating nevus (n = 2), pigmented spindle cell nevus (n = 2), and proliferative nodule in congenital pattern nevus (n = 2).

Table 2.

40 CpG probes in the melanoma diagnostic classifier

CpG ID	Gene(s)	Gene name	Chr	Location relative to gene[1]	Location relative to CpG Island	Enhancer	Regulatory Feature[2]	Methylation: melanomas vs. nevi	Mean β melanomas	Mean β nevi	p value[3]
cg02936049	*ZBTB38*	Zinc Finger And BTB Domain Containing 38	3	5'UTR	--	Yes		hyper	0.6439	0.2438	1.79E-24
cg19352038	*PAX3; CCDC140*	Paired Box 3; Coiled-Coil Domain Containing 140	2	TSS1500; 5'UTR	S_Shore	Yes		hyper	0.7275	0.2998	5.41E-24
cg16325502	*CCDC140*	Coiled Coil Domain Containing 140	2	5'UTR	N_Shore			hyper	0.6445	0.1971	1.46E-23
cg05787556	*TLX3*	T-Cell Leukemia Homeobox 3	5	TSS1500	Island	Yes		hyper	0.5660	0.1849	2.97E-23
cg12993163	*SHOX2*	Short Stature Homeobox 2	3	Body	Island		UCTS	hyper	0.5156	0.1211	3.18E-23
cg08697503	*CCDC140*	Coiled-Coil Domain Containing 140	2	5'UTR	N_Shore			hyper	0.6263	0.2026	4.76E-23
cg18077971	*PAX3; CCDC140*	Paired Box 3; Coiled-Coil Domain Containing 140	2	TSS1500; 5'UTR	S_Shore	Yes		hyper	0.6626	0.2259	1.44E-22
cg06215569	*ALX3*	ALX Homeobox 3	1	Body	Island	Yes		hyper	0.6228	0.1524	9.07E-22
cg16919569	*NBLA00301; HAND2*	(HAND2-AS1) HAND2 Antisense RNA 1 (Head To Head); Heart And Neural Crest Derivatives Expressed 2	4	Body; TSS1500	Island			hyper	0.6748	0.3470	1.74E-21
cg13164157	*PROM1*	Prominin 1 (CD133)	4	5'UTR	Island	Yes	UCTS	hyper	0.4445	0.0586	3.77E-21
cg07230581	*OPCML*	Opioid Binding Protein/Cell Adhesion Molecule-Like	11	TSS1500	--			hypo	0.4214	0.7547	6.71E-21
cg00387964	*SORCS2*	Sortilin Related VPS10 Domain Containing Receptor 2	4	Body	S_Shelf		Uncl	hypo	0.3893	0.8097	1.05E-20
cg03315407	*ANKH*	ANKH Inorganic Pyrophosphate Transport Regulator	5	Body	--	Yes	Uncl	hypo	0.2717	0.6184	2.04E-20

CpG ID	Gene(s)	Gene name	Chr	Location relative to gene[1]	Location relative to CpG Island	Enhancer	Regulatory Feature[2]	Methylation: melanomas vs. nevi	Mean β melanomas	Mean β nevi	p value[3]
cg02744046	*LIPC*	Lipase C, Hepatic Type	15	Body	--			hyper	0.6004	0.2332	2.24E-20
cg13019491	*SIX6*	SIX Homeobox 6	14	Body	Island			hyper	0.5128	0.1094	2.54E-20
cg17918270	*MYT1L*	Myelin Transcription Factor 1 Like	2	Body	--			hypo	0.5044	0.8731	6.10E-20
cg18689332	*TBX5*	T-Box 5	12	Body	N_Shore	Yes		hyper	0.7265	0.3632	6.29E-20
cg08337633	*VOPP1*	Vesicular, Overexpressed In Cancer, Prosurvival Protein 1	7	Body	--	Yes	PA	hypo	0.3099	0.6939	1.21E-19
cg15849098	*GIMAP7*	GTPase, IMAP Family Member 7	7	TSS200	--		UCTS	hypo	0.3606	0.6898	1.54E-19
cg26967305	*KREMEN1*	Kringle Containing Transmembrane Protein 1	22	3'UTR	--		UCTS	hypo	0.4830	0.7867	1.59E-19
cg03874199	*HOXD12*	Homeobox D12	2	TSS200	Island			hyper	0.5570	0.1707	3.22E-19
cg10559416	*CYTIP*	Cytohesin 1 Interacting Protein	2	1st Exon	--			hypo	0.5015	0.8105	1.19E-18
cg14064356	*CCDC140*	Coiled-Coil Domain Containing 140	2	5'UTR	N_Shore	Yes		hyper	0.6245	0.2139	1.70E-18
cg22322562	*NRXN1*	Neurexin 1	2	Body	--			hyper	0.6634	0.3041	3.79E-18
cg02468320	*CACNA1C*	Calcium Voltage-Gated Channel Subunit Alpha1 C	12	Body	--	Yes		hypo	0.4413	0.7889	4.40E-18
cg04499514	*C3AR1*	Complement Component 3a Receptor 1	12	TSS200	--		PA	hypo	0.4203	0.7683	2.69E-17
cg07569216	*ONECUT1*	One Cut Homeobox 1	15	Body	N_Shore			hyper	0.6641	0.3067	3.29E-17
cg07637837	*MBP*	Myelin Basic Protein	18	5'UTR	Island			hypo	0.4298	0.7612	3.49E-17
cg08898055	*RASGEF1C*	RasGEF Domain Family Member 1C	5	5'UTR	--	Yes		hyper	0.5153	0.1971	3.59E-17
cg09476130	*CCDC19*	(CFAP45) Cilia And Flagella Associated Protein 45	1	TSS200	Island	Yes		hyper	0.6648	0.3535	4.52E-17
cg15158847	*FAIM3*	Fas Apoptotic Inhibitory Molecule 3; (alias FCMR) Fc	1	5'UTR; 1stExon	--		Uncl	hypo	0.4876	0.7843	4.65E-17

CpG ID	Gene(s)	Gene name	Chr	Location relative to gene[1]	Location relative to CpG Island	Enhancer	Regulatory Feature[2]	Methylation: melanomas vs. nevi	Mean β melanomas	Mean β nevi	p value[3]
		Fragment Of IgM Receptor 1stExon									
cg18851100	*SHANK3*	SH3 And Multiple Ankyrin Repeat Domains 3	22	Body	Island			hyper	0.6274	0.3162	8.95E-17
cg07553475	*FLJ22536*	CASC15; Cancer Susceptibility Candidate 15 (Non-Protein Coding)	6	TSS1500	Island			hyper	0.5285	0.1341	5.39E-16
cg15536663	*EPB41L4A*	Erythrocyte Membrane Protein Band 4.1 Like 4A	5	Body	--	Yes		hypo	0.3481	0.6444	7.30E-16
cg06573459	*SGEF*	(ARHGEF26) Rho Guanine Nucleotide Exchange Factor 26	3	Body	S_Shore		UCTS	hyper	0.5123	0.1580	9.35E-16
cg03653573	*C5orf56*	Chromosome 5 Open Reading Frame 56	5	Body	--		PA	hypo	0.3512	0.6451	2.12E-15
cg18098839	*GOLIM4*	Golgi Integral Membrane Protein 4	3	Body	--	Yes		hypo	0.3378	0.6652	9.51E-15
cg17889682	*DYNC1I1*	Dynein Cytoplasmic 1 Intermediate Chain 1	7	5'UTR	S_Shore	Yes		hyper	0.6412	0.3127	1.70E-14
cg08757862	*TLR1*	Toll Like Receptor 1	4	TSS1500	--		PA	hypo	0.5317	0.8120	2.58E-14
cg12423733	*MAS1L*	MAS1 Proto-Oncogene Like, G Protein-Coupled Receptor	6	1st Exon	--			hypo	0.4461	0.7019	5.69E-12

[1] TSS; transcription start site, UTR; untranslated region.

[2] UCTS, unclassified cell type-specific; Uncl, unclassified; PA, promoter-associated.

[3] Wilcoxon p value for mean β in melanomas versus nevi.